

Supplementary Materials for

Unidirectional rotating molecular motors dynamically interact with adsorbed proteins to direct the fate of mesenchymal stem cells

Qihui Zhou, Jiawen Chen, Yafei Luan, Petteri A. Vainikka, Sebastian Thallmair, Siewert J. Marrink, Ben L. Feringa*, Patrick van Rijn*

*Corresponding author. Email: b.l.feringa@rug.nl (B.L.F.); p.van.rijn@umcg.nl (P.v.R.)

Published 29 January 2020, *Sci. Adv.* **6**, eaay2756 (2020)
DOI: 10.1126/sciadv.aay2756

This PDF file includes:

Fig. S1. Altered cell behavior induced by molecular motion–mediated protein layer restructuring.

Fig. S2. Proliferation capacity of MSCs on molecular motor–functionalized surfaces in static and rotating mode upon protein adhesion.

Fig. S3. Immunofluorescence analysis of cell morphology during osteogenic differentiation of MSCs on dynamic and static molecular motor–functionalized surfaces.

Fig. S4. Protein adhesion and structural integrity mediated by molecular motion and UV irradiation.

Fig. S5. MD simulations of protein–molecular motor interactions and motion-induced structural deformation.

Fig. S6. AFM analysis of motion-induced alterations to structural alterations of protein adhesion layers.

Fig. S7. Physicochemical influences on the morphology of protein adhesion layers.

Table S1. Primer sequences of human-specific genes used for qRT-PCR.

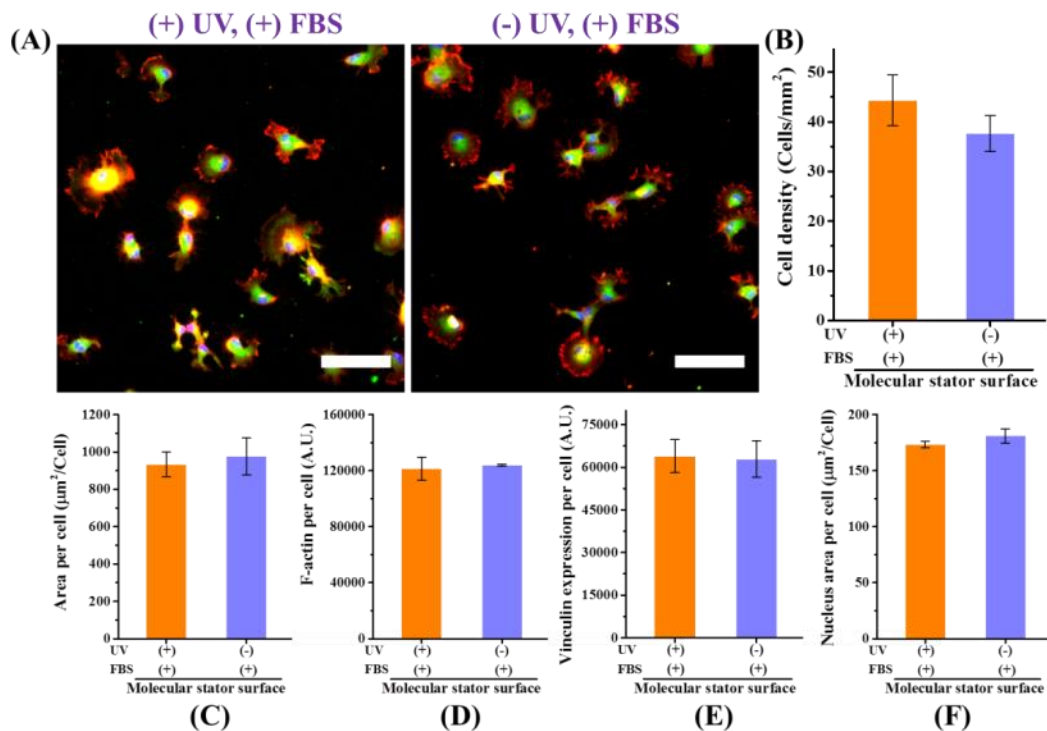


Fig. S1. Altered cell behavior induced by molecular motion-mediated protein layer restructuring.

(A) Fluorescent images of hBM-MSCs cultured on molecular stator surfaces for 12 h. Scale bar: 100 μm. Red: F-actin; Green: vinculin; Blue: Nucleus. (B) cell density, (C) area per cell, (D) F-actin per cell, (E) vinculin expression per cell, (F) nucleus area per cell on molecular stator surfaces with (+) or without (-) UV treating ($\lambda_{\max} = 365$ nm) (N=3).

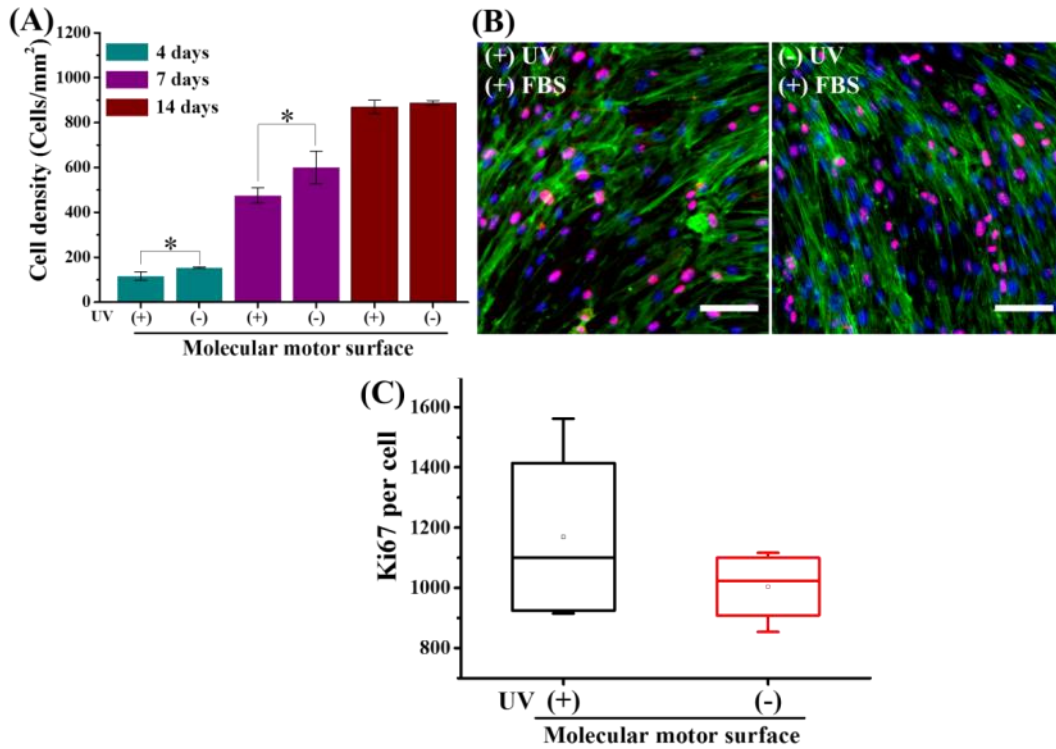


Fig. S2. Proliferation capacity of MSCs on molecular motor–functionalized surfaces in static and rotating mode upon protein adhesion. (A) Cell density on molecular motor surfaces with different cell culture time (N=3) with (+) or without (-) UV treating ($\lambda_{\max} = 365$ nm). (B) Fluorescent images of hBM-MSCs cultured on molecular motor surfaces for 7 days. Scale bar: 100 μm. Pink: Ki67; Green: F-actin; Blue: Nucleus. (C) Ki67 per cell on molecular motor surfaces with different conditions for 7 days (N=3). Data reported as mean ± standard deviation (SD). (*p < 0.05)

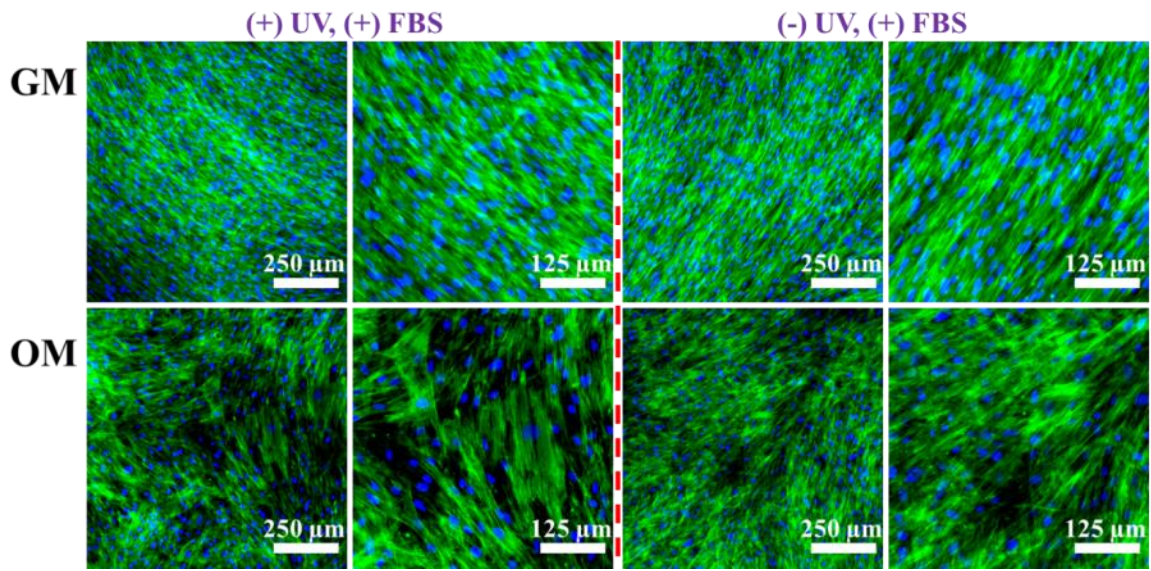


Fig. S3. Immunofluorescence analysis of cell morphology during osteogenic differentiation of MSCs on dynamic and static molecular motor-functionalized surfaces. Fluorescent images of hBM-MSCs cultured on molecular motor surfaces with different cell mediums with (+) or without (-) UV treating ($\lambda_{\text{max}} = 365 \text{ nm}$) for 14 days. Green: F-actin; Blue: Nucleus. GM means growth medium; OM means osteogenic differentiation medium.

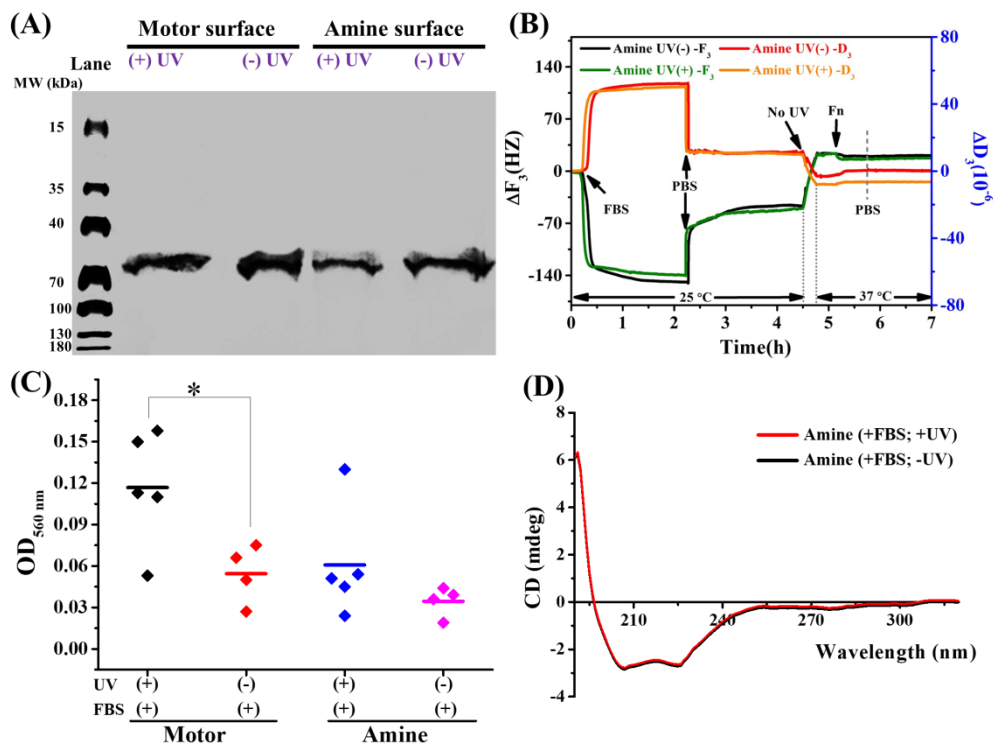


Fig. S4. Protein adhesion and structural integrity mediated by molecular motion and UV irradiation. (A) SDS-PAGE banding patterns of FBS protein adsorbed on molecular motor and amine surfaces at different conditions. (B) Protein adsorption on the amine surface with different conditions measured by QCM-D. (C) Protein mass from FBS adsorbed on molecular motor and amine surfaces with different conditions measured by the bicinchoninic acid (BCA) assay (* $p < 0.05$). (D) CD spectra of protein from BSA adsorbed on and the amine surface with different conditions. Data reported as mean \pm standard deviation (SD). ((+) with, (-) without UV treating, $\lambda_{\text{max}} = 365 \text{ nm}$)

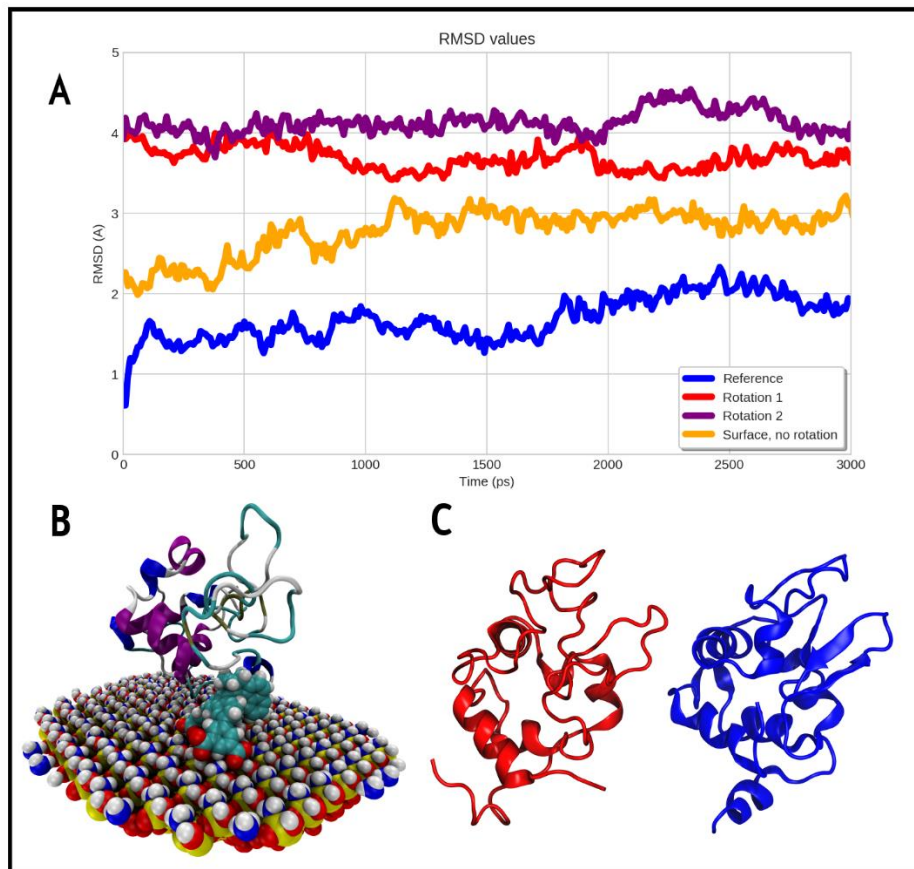


Fig. S5. MD simulations of protein–molecular motor interactions and motion-induced structural deformation. (A) RMSD values for the protein experiencing a single rotation (purple), protein experiencing three different rotations (red), protein on an inactive surface (yellow), and protein in pure water (blue). (B) Snapshot revealing direct protein – motor interaction. (C) Differences in secondary structure between the protein on an active surface (red), and on an inactive surface (blue).

Molecule Motor Surface

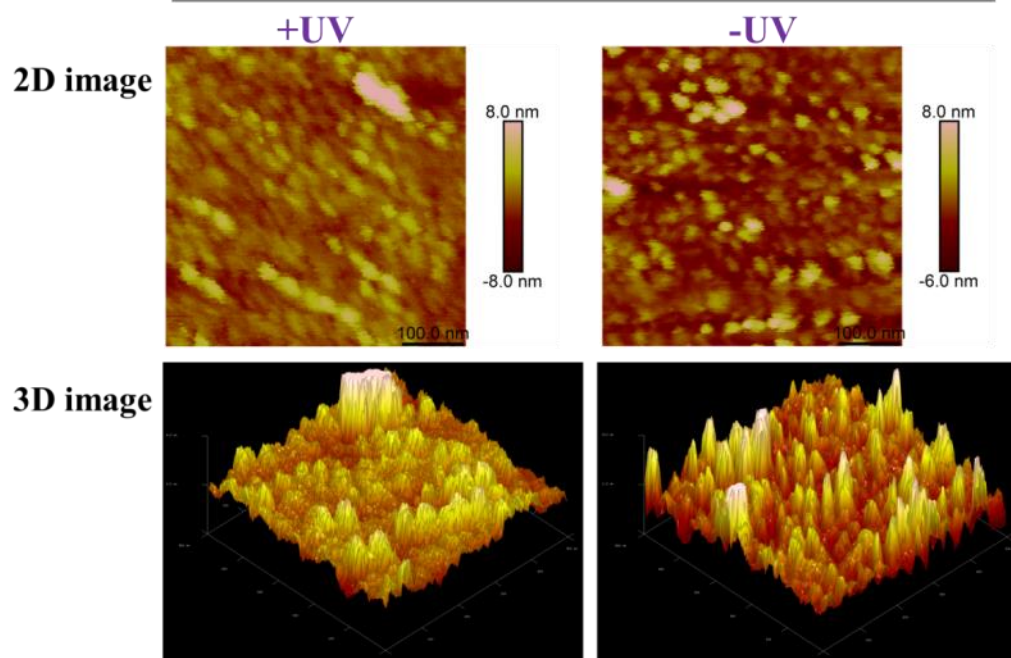


Fig. S6. AFM analysis of motion-induced alterations to structural alterations of protein adhesion layers. AFM images of adsorbed BSA proteins on the dynamic and static molecular motor surfaces.

Table S1. Primer sequences of human-specific genes used for qRT-PCR.

Genes	5'-3'	Primers
36B4	Forward	AACGGGTACAAACGAGTC
	Reverse	AGATGGATCAGCCAAGAAG
Nanog	Forward	TCCAACATCCTGAACCTCAGC
	Reverse	AGGCATCCCTGCGTCACA
OCT4	Forward	GGGGTTCTATTTGGGAAGGTAT
	Reverse	GCCGCAGCTTACACATGTTC
OPN	Forward	ACTCGAACGACTCTGATGATGT
	Reverse	GTCAGGTCTGCGAAACTTCTTA

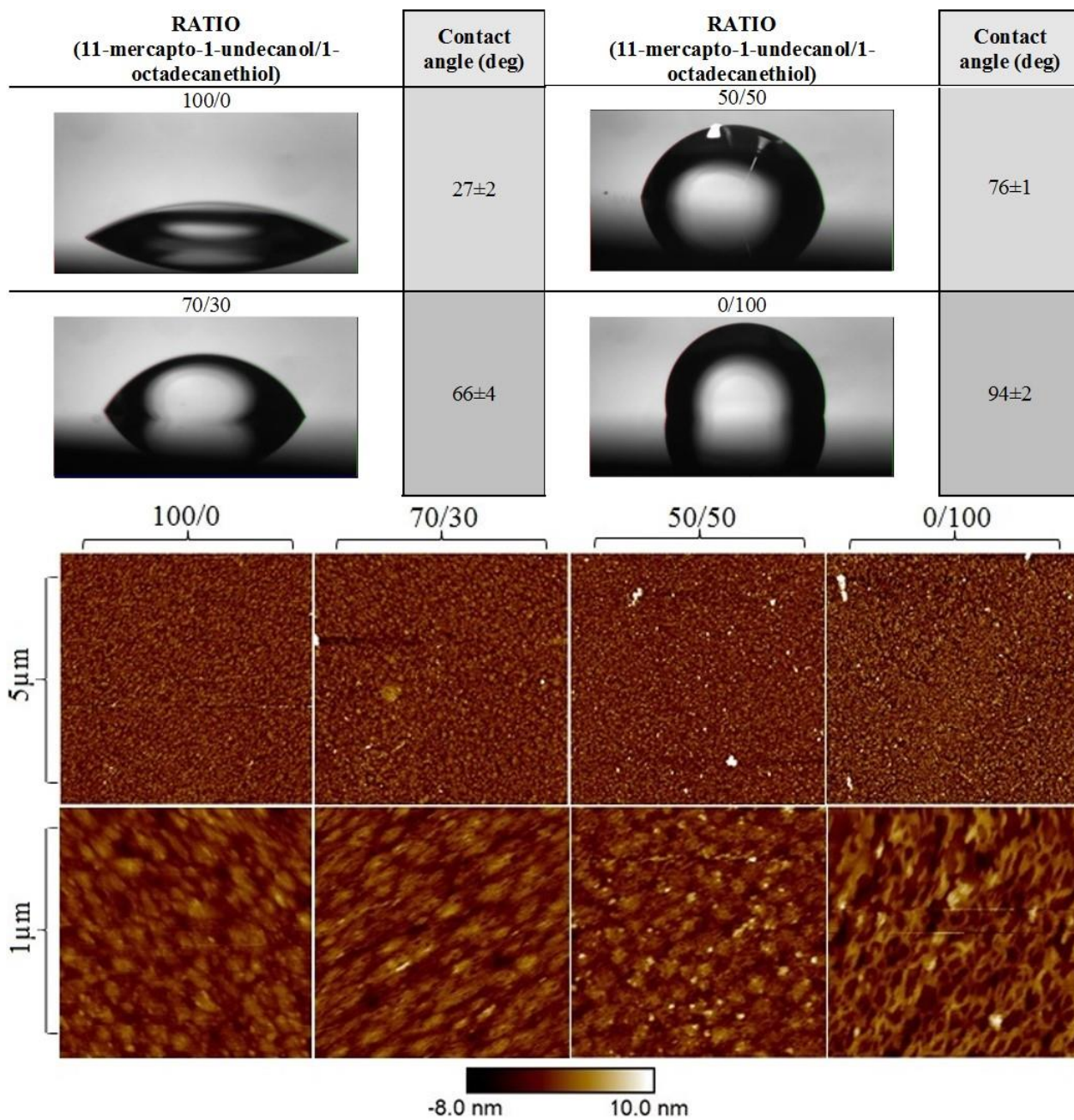


Fig. S7. Physicochemical influences on the morphology of protein adhesion layers. AFM images of adsorbed BSA proteins on surfaces of different wettability of which it is known that the hydrophobic surface induces better osteogenesis.